Aerosol Science and Technology

ISSN: (Print) (Online) Journal homepage: https://www.tandfonline.com/loi/uast20

Size-dependent depositional loss of inorganic, organic, and mixed composition particles to Teflon chamber walls under various environmental and chemical conditions

Adrianne Nakagawa, Kelvin H. Bates & Tran B. Nguyen

To cite this article: Adrianne Nakagawa, Kelvin H. Bates & Tran B. Nguyen (18 Jan 2024): Size-dependent depositional loss of inorganic, organic, and mixed composition particles to Teflon chamber walls under various environmental and chemical conditions, Aerosol Science and Technology, DOI: 10.1080/02786826.2023.2298219

To link to this article: https://doi.org/10.1080/02786826.2023.2298219

AEROSOL SCIENCE AND TECHNOLOGY
https://doi.org/10.1080/02786826.2023.2298219

Size-dependent depositional loss of inorganic, organic, and mixed composition particles to Teflon chamber walls under various environmental and chemical conditions

Adrianne Nakagawa[a], Kelvin H. Bates[b,c*], and Tran B. Nguyen[c]

[a]Department of Chemistry, University of California Davis, Davis, California, USA; [b]Center for the Environment, Harvard University, Cambridge, Massachusetts, USA; [c]Department of Environmental Toxicology, University of California Davis, Davis, California, USA

ABSTRACT

Corrections for first-order particle losses to Teflon chamber walls are important sources of uncertainty in experimental studies of particle formation and aging. Particle size distributions and environmental factors significantly influence wall loss corrections; thus, it is important to characterize size-dependent particle loss profiles under myriad experimental conditions that may alter deposition rates. This work investigated size-dependent loss coefficients of inorganic (ammonium sulfate, AS), organic (sorbitol, $C_6H_{14}O_6$), and mixed composition (AS + sorbitol, 1:1 by mole) particles to a Teflon chamber under varying chamber temperature (20–40 °C), relative humidity (RH, <10–80%), illumination (dark vs. 100% chamber lights), particle water (crystalline vs. deliquesced vs. metastable), and chamber usage history conditions (clean chamber vs. following chemical experiments). It was found that temperature and lights had negligible to minor effects on loss rates for all particles, while RH, particle water, and chamber usage history each had major effects under all tested conditions. Particle wall loss rates were higher under humid than dry conditions, and higher for deliquesced particles than for dry particles at similar RH. Chemical conditions that introduced acidic species to chamber walls the day prior to a wall loss experiment were responsible for uncertainties of up to ~50% in wall loss rate profiles, despite recommended chamber flushing regimens. These data suggest that sensitive OA formation or aging experiments may consider obtaining same-day wall loss profiles from the target experiment. Otherwise, size-dependent corrections for particle wall loss should consider particle composition, particle water, RH, wall usage history, and possibly illumination conditions.

ARTICLE HISTORY
Received 7 August 2023
Accepted 15 December 2023

EDITOR
Jim Smith

1. Introduction

Atmospheric simulation chambers (i.e., "smog" chambers) are often used to study the chemical and physical transformations of aerosol particles. Although atmospheric simulation chambers can be constructed from various materials (e.g., stainless steel, polymer plastics, quartz, glass), a majority of the large chambers that are run in batch mode are constructed from optically transparent Teflon® (polytetrafluoroethylene) polymer film due its characteristics of light transmissibility, durability, and chemical inertness. Particle interactions with Teflon chamber walls are a significant source of uncertainty in organic aerosol formation and aging experiments (Wang et al. 2018a), and particle wall losses can be affected by the various disadvantageous qualities of Teflon films in addition to gravitational sedimentation, diffusion, and other universal chamber effects (Corner and Pendlebury 1951; Crump and Seinfeld 1981; Crump, Flagan, and Seinfeld 1982; McMurry and Rader 1985). For example, Teflon is an insulating material that holds electrostatic charges, and electrostatic effects contribute to depositional wall losses of particles in the 0.05-1.0-μm diameter range (McMurry and Grosjean 1985; Pierce et al. 2008). Teflon walls can also retain a usage "history" of experiments performed in the chamber, as mechanical cleaning of Teflon chamber walls is often infeasible. This has been documented to affect wall losses of vapors (Loza et al. 2010; Shao et al.

CONTACT Tran B. Nguyen tbn@ucdavis.edu Department of Environmental Toxicology, University of Colorado CIRES, NOAA CSL, 325 Broadway, Boulder, CO 80305-3337, USA.
*Current affiliation NOAA Chemical Sciences Laboratory, Earth System Research Laboratories, & Cooperative Institute for Research in Environmental Sciences, University of Colorado, Boulder, Colorado, USA.

Supplemental data for this article can be accessed online at https://doi.org/10.1080/02786826.2023.2298219.

2022) and may logically extend to wall losses of particles although it has not yet been shown explicitly. Moreover, in sufficiently humid conditions, the surface of Teflon chambers can be coated with a liquid sublayer (Huang et al. 2018), further suggesting that interactions between chamber walls and particles of different composition and phase are likely complex.

Wall loss rates of particle numbers (N) in chambers have been classically expressed as an apparent first-order loss through the particle diameter (D_p)-dependent wall loss coefficient β (Crump, Flagan, and Seinfeld 1982):

$$\frac{dN}{N} = -\beta(D_p)dt$$

While β is influenced by kinetic parameters for eddy-diffusion or coagulation (Charan et al. 2018; Nah et al. 2017; Wang et al. 2018a), the observable losses of particles can be extracted as a time-dependent exponential decay at each D_p size bin. Some early chamber experimental efforts either ignored particle wall losses (Stern et al. 1987) or focused on size-independent wall loss rates using monodisperse aerosol (Chen, Yeh, and Cheng 1992; Ingebrethsen and Sears 1989; Offermann et al. 1985; Okuyama et al. 1977; Pandian and Friedlander 1988), although even the earliest wall loss parameterizations noted the size dependence of diffusional and gravitational particle wall loss rates in stirred rectangular vessels (Corner and Pendlebury 1951). These early parameterizations were eventually generalized to chambers of other shapes (Crump and Seinfeld 1981), modified to include the electrostatic effects of Teflon (McMurry and Grosjean 1985; McMurry and Rader 1985), and validated experimentally in numerous chambers (Crump, Flagan, and Seinfeld 1982; Okuyama et al. 1986; Park et al. 2001; Takekawa, Minoura, and Yamazaki 2003).

Presently, there are a number of particle wall loss corrections suggested and applied in the scientific literature: (A) a particle size-independent correction based on total particle mass concentration (Pathak et al. 2007; Wang et al. 2014; Weitkamp et al. 2007); (B) a particle size-dependent correction based on either an average β loss profile (e.g., Fry et al. 2014; Keywood et al. 2004; McMurry and Grosjean 1985; Ng et al. 2007), a β loss profile dependent on certain parameters (e.g., particle loading; Schwantes et al. 2019) or experiment-dependent β loss profiles (e.g., Wang et al. 2018b); and (C) a size-independent particle composition-based correction using the ratio of organic aerosol either to sulfate aerosol measured by an aerosol mass spectrometer (Henry and Donahue 2012; Hildebrandt, Donahue, and Pandis 2009; Loza et al. 2012) or to black carbon measured by an aethalometer (Hennigan et al. 2011). However, Wang et al. (2018a) demonstrated how size-independent loss rate constants introduce significant error into wall loss corrections especially for size distributions containing ultrafine particles ($D_p < 100$ nm) due to coagulation. Furthermore, the authors found that particle wall losses can vary both between and within experiments, yet a systematic evaluation of size-dependent particle wall losses under the large array of potential experimental conditions tested in atmospheric simulation chambers is not yet available in the literature.

This study examines particle wall losses in a Teflon chamber for inorganic (ammonium sulfate, AS), organic (sorbitol), and mixed composition (AS + sorbitol at 1:1 molar ratio) particles as a function of chamber relative humidity (RH), chamber temperature (T), particle water (dry/crystalline or wet/hydrated), illumination from chamber lights, and lastly, chamber usage history with respect to chemical oxidation experiments. We did not include a coagulation correction for experimentally derived β (D_p) profiles as we only consider relative trends in β (D_p) profiles. Additionally, a majority of the observed differences in particle wall loss rates are in the larger D_p range where coagulation is less important and where the correction to mass concentration has the potential for the highest errors.

2. Experimental

2.1. Chamber design and use

Wall loss experiments were conducted in a rectangular prism 10 m^3 environmental chamber (surface area, 28 m^3) constructed from Dupont Teflon-FEP with a thickness of 2 mil (0.002 inch). The suspended bag is housed in a climate-controlled enclosure with UV-reflective interior siding. Two sets of Sylvania 40 W broadband blacklights (peak wavelength, 350 nm) are installed along opposite walls of the enclosure with each set comprised of thirty-six bulbs. The mixing method for this chamber consists of ten rapid pulses of pressurized purified air. The pulsed air is injected by toggling a manual actuator between open/closed for about 1–2 s on each pulse.

We completed these experiments over a several month period during which the chamber was also being used to conduct oxidation experiments involving ozone, nitrate radicals, sulfur dioxide and/or terpenes. Prior to each wall loss experiment, we flushed the chamber overnight with dry purified air at 100 L

min^{-1} ensuring at least 17 h of cleaning and more than 7 chamber volumes of flushing air between any other usage. This cleaning method is consistent with guidelines and standard operating procedures for chambers of similar size (Bell, Doussin, and Hohaus 2023; Ma et al. 2022; Wu et al. 2007). In some cases, the chamber was photochemically cleaned prior to overnight flushing by irradiation of 4 – 10 ppm H_2O_2 while heating to ~40 °C without particles or organics present. In general, starting particle concentrations were below 15 cm^{-3} (0.20 μg m^{-3}), and for those experiments with higher starting concentrations, we determined the chamber had been flushed for at least two consecutive days or more between uses; thus, we do not consider the higher concentrations to be evidence of chamber contamination.

2.2. Experimental design

We conducted a total of 26 unique particle wall loss experiments using either AS (≥99.0%, Sigma Aldrich), sorbitol (>97.0%, Tokyo Chemical Industry), or a 1:1 molar mixture of AS and sorbitol. The seed particles are representative compounds for inorganic, organic, and mixed composition species, respectively. For each of the three different seed compositions, we systematically varied the experimental conditions in the chamber with respect to RH, dry/wet seed injection, temperature, and illumination. Table 1 shows the different experimental combinations, and it also indicates which experiments were preceded by an oxidation experiment on the previous day.

In a typical wall loss experiment, the chamber was controlled to the desired temperature and humidity, and both temperature and humidity were monitored throughout the experiment with a membrane probe (Vaisala Inc.) calibrated with saturated salt solutions. After sealing off the chamber, atomization of the seed solution with UHP N_2 gas (Linde) proceeded for 25 min followed by bursts of pressurized purified air to mix the chamber. The atomized particles passed through a ^{210}Po neutralizer to ensure a consistent charge distribution and a charcoal denuder to remove water vapor and gas-phase contaminants. Particles were typically injected in the range of 1 – 3 × 10^5 cm^{-3}. To ensure similar particle loading during injection, we prepared aqueous solutions for each of the seed compositions at total concentrations of 0.02 M using ultrapure water. For experiments with wet injection, the particles were also passed through a heated wet-wall denuder to achieve particle deliquescence. Mass concentrations for injected particles are

Table 1. List of unique particle wall loss experiments performed.

Seed Composition	RH	Dry/wet injection	Temp. (°C)	Dark/ Lights	Prev. day oxidation expt.	Repeated
AS	<10%	dry	20	Dark	N	N
AS	<10%	dry	30	Dark	N	N
AS	<10%	dry	40	Dark	N	N
AS	<10%	dry	40	Dark	Y	N
AS	60%	dry	20	Dark	N	N
AS	60%	dry	20	Light	N	N
AS	60%	wet	20	Dark	N	Y
AS	80%	wet	20	Dark	N	N
AS + Sorb	<10%	dry	20	Dark	N	N
AS + Sorb	60%	dry	20	Dark	N	N
AS + Sorb	60%	wet	20	Dark	N	N
AS + Sorb	80%	wet	20	Dark	N	N
Sorb	<10%	dry	20	Dark	N	N
Sorb	<10%	dry	20	Light	N	Y
Sorb	<10%	dry	20	Light	Y	N
Sorb	<10%	dry	30	Dark	N	N
Sorb	<10%	dry	30	Dark	Y	N
Sorb	<10%	dry	40	Dark	N	N
Sorb	60%	dry	20	Dark	N	Y
Sorb	60%	dry	20	Light	N	N
Sorb	60%	wet	20	Dark	N	N
Sorb	60%	wet	20	Dark	Y	N
Sorb	60%	wet	20	Light	N	Y
Sorb	60%	wet	20	Light	Y	N
Sorb	80%	wet	20	Dark	N	Y
Sorb	80%	wet	20	Dark	Y	N

Seed particle compositions tested include ammonium sulfate (AS), sorbitol (Sorb), and a molar equivalent mixture of both (AS + Sorb). Relative humidity (RH) values represent ranges that are ±5%. Temperature values (±1°C) can increase *ca.* 3 °C when 100% lights are turned on. Dry injection is a direct atomization into the chamber, while wet injection is an atomization through a heated wet wall denuder. Oxidation experiments performed include ozone and nitrate radical oxidations of terpenes (α- and β-pinene, ocimene, sabinene, etc.) and photooxidation of sulfur dioxide (SO_2). Repeated experiments have been replicated 2–3 times.

in the range of 200–500 μg m^{-3} with a mean D_p of 50–90 nm depending on particle water content. If the experiment was performed under illumination, all light bulbs were turned on immediately following mixing air and left on for the duration of the experiment. The timescale of mixing for particles in the chamber is <5 min with mixing air and >30 min without.

We monitored particle losses using a scanning mobility particle sizer (SMPS, TSI 3080 electrostatic classifier coupled to a TSI 3772 condensation particle counter) with diameter cutoffs set at 15 and 670 nm and a sampling frequency of 5 min. Wall loss experiments ranged from 3 to 10 h in length, with the experiment start time demarcated by the final injection of mixing air for dark experiments or by turning on lights for illuminated experiments. Given the sampling frequency, this allowed us to acquire at least 36 scans for analyzing wall loss rates. Particle wall loss coefficients $\beta(D_p)$ presented in Section 3 are calculated by fitting particle number concentration data in each size bin to an exponential decay function using a custom Matlab program.

3. Results and discussion

3.1. Determining uncertainty of wall loss profiles

Figure 1 shows the particle number distribution and volume concentration data, extracted β (Dp) values and fitted wall loss profile, and the applied corrections for a representative particle wall loss experiment using dry sorbitol particles. First, it is important to establish the baseline uncertainty for repeated experiments. For experiments performed identically with similar wall usage history, we determined that $\beta(D_p)$ profiles are highly reproducible (Figure S1); the baseline uncertainty (1 standard deviation of repeated experiments) for extracting a wall loss profile is 4–8% across the entire experimental D_p range and 2–9% in the range of $D_p >$ 100 nm. While this repeatability error is relatively small, it may pose a challenge for experiments requiring greater precision, such as secondary organic aerosol (SOA) experiments where the mass gain or loss is slow. Furthermore, the associated errors in the correction will increase with experimental time such that $\beta(D_p)$ profiles inherently produce more

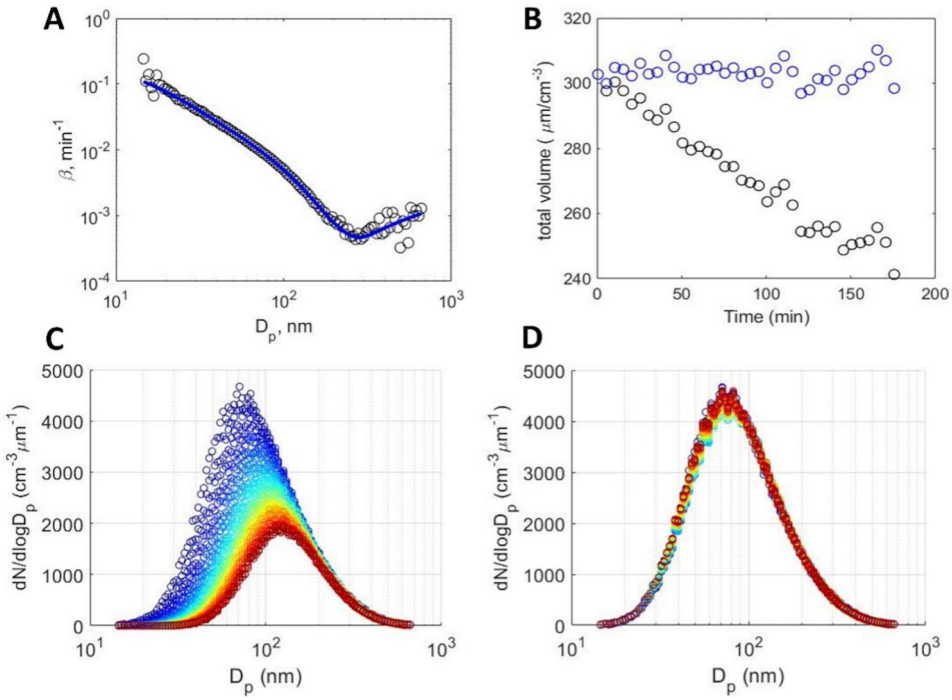

Figure 1. Representative particle wall loss experiment with sorbitol particles under dry conditions at 20 °C nominal temperature in the dark. Panel (a) shows the $\beta(D_p)$ profile as raw extracted data points (black open circles) and a fitted curve (blue line). Panel (b) shows the total particle volume throughout the experiment as uncorrected data (black) and corrected using the $\beta(D_p)$ profile shown in (a) (blue). Panel (c) shows the uncorrected particle number distribution throughout the D_p range as the experiment proceeds (gradient blue to red, beginning to end). Panel (d) shows the particle number distribution of the experiment as corrected using the β (D_p) profile shown in (a).

uncertainty in longer experiments compared to shorter ones. The repeatability errors may stem from computational fits and/or any of the numerous experimental preparations from setting the chamber environmental conditions to injecting the particles. The results obtained from varying experimental parameters in this work will be benchmarked against the baseline uncertainty to understand the significance of the deviations.

3.2. Effects of humidity and particle hydration

Chamber RH has a large impact on wall loss profiles for all particle compositions, much higher than the baseline uncertainty, but the effects depend on particle water content (Figure 2). We uniformly observe that all particles undergo slower wall loss at lower RH. In the dry (RH < 10%) environment the wall loss profile

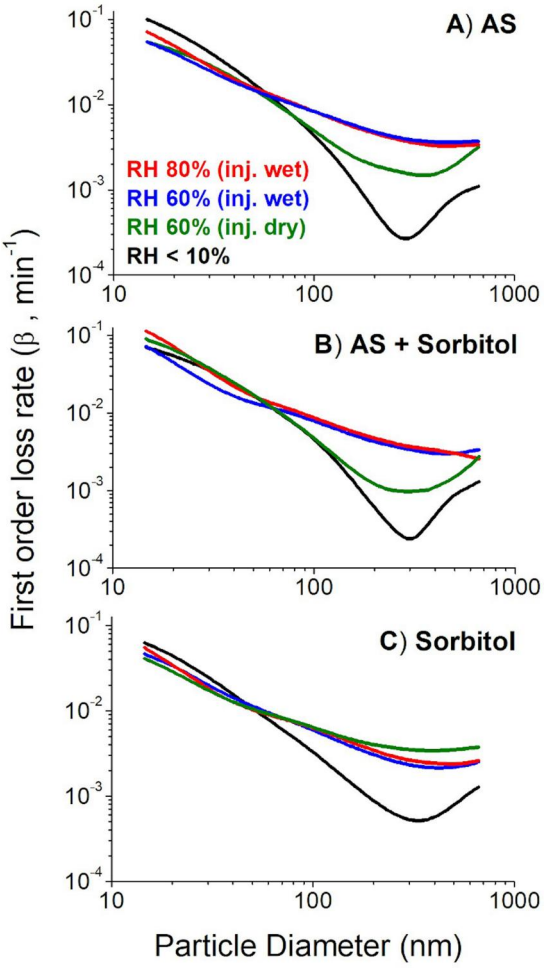

Figure 2. The $\beta(D_p)$ profile of sorbitol, ammonium sulfate (AS), and mixed AS + sorbitol particles at different relative humidity (RH) in the dark. AS-based seed particles may be injected as hydrated particles (wet) or crystalline particles (dry) at 40% < RH < 80% due to its deliquescence and efflorescence behavior. Sorbitol particles have continuum hydration behavior.

for AS particles (Figure 2a) exhibits a relatively sharp minimum, as smaller diameter particles are lost quickly to diffusion while larger diameter particles are lost to sedimentation in a batch mode reactor (Crump, Flagan, and Seinfeld 1982). At RH 80%, AS particles are fully deliquesced (Biskos et al. 2006) and it can be assumed that the chamber walls with previously-deposited particles contain a film of water. These assumptions are consistent with the observed dampening of the minimum, higher overall loss rates, and slightly lower diffusional losses in the low diameter range when the particle is fully deliquesced. At RH 60%, AS particles can be either in a dry crystalline or a hydrated metastable state, the former if particles are injected dry and the latter if particles are injected "wet" past the deliquescence RH value using a wet wall denuder (typically held at RH > 95% when heated). We find that hydrated AS at RH 60% has a nearly identical $\beta(D_p)$ profile to fully deliquesced particles at RH 80%. However, loss rates at RH 60% are much lower for dry particles than wet ones, with a profile between that of the RH <10% and the RH 80% scenarios. We also note that the size distributions are consistent with their corresponding $\beta(D_p)$ profiles insofar as AS particles at RH 60% had a similar size distribution to dry crystalline AS particles in the RH <10% environment only when injected dry (Figure S2). When injected wet, the particles had distinctly larger mean diameters than either the dry AS at RH <10% or the dry-injected AS at RH 60%.

Interestingly, we found that the mixed composition particles (Figure 2b) behaved nearly identically to pure AS with respect to wall depositional losses, implying that, for a hygroscopic organic such as sorbitol, AS likely controls the particle water when the molar ratio of organic to inorganic is equal. This is consistent with the small deviations in deliquescence RH values measured for 1:1 mixtures of AS with other water soluble organics (Parsons, Knopf, and Bertram 2004, and references therein), all of which are higher than the 60% RH threshold tested here. It appears that, for AS and AS + sorbitol systems, particles containing liquid water reach a maximum $\beta(D_p)$ profile. It is not clear how these results extend to mixtures of AS with more viscous organics, such as SOA from the oxidation of certain aromatics or terpenoids (Reid et al. 2018). Nevertheless, these results show that particle water plays a major role in wall deposition patterns, not just environmental RH. Furthermore, it is possible for particles to be hydrated differently than the walls at a particular RH, which should be

considered when determining the most appropriate particle wall loss correction profiles and methods.

On the other hand, pure sorbitol particles (Figure 2c) neither deliquesce nor effloresce; they uptake water continuously at the full RH range but contain less than 10% water by mole until RH 40% (Peng, Chow, and Chan 2001). In congruence, the $\beta(D_p)$ profile of sorbitol at dry conditions is similar in magnitude to mixed composition particles but with a less sharp minimum. As expected, and in contrast to AS particles, we found that dry vs. wet injections of sorbitol made little difference in its wall depositional loss profile, and again, the size distribution of sorbitol particles at RH 60% is consistent with the corresponding $\beta(D_p)$ profile in that particles, whether injected dry or wet, were distinctly larger than dry sorbitol particles (Figure S3). Additionally, at higher RH conditions (60–80%), sorbitol particles contain approximately 20–40% water by mole, and we observed no significant differences in loss profiles at these thresholds. It is possible that the $\beta(D_p)$ profile for sorbitol particles is more sensitive in the low to moderate RH range (10% < RH < 60%) that was not tested here.

The trends of enhanced particle wall loss with higher RH and particle liquid water suggest that particle deposition in humid conditions is both a function of the particle's properties and the characteristics of the Teflon film at that particular RH. While electrostatic effects should be dampened instead of exacerbated with higher RH, water vapor can increase particle size to increase sedimentation (Kim et al. 2023). Additionally, if we consider the treatment of dry deposition to wet surfaces in the environment (Emerson et al. 2020), the surface layer characteristics may change the efficiency with which particles are intercepted by the surface. Thus, for higher RH, the water layer on Teflon chamber walls likely increases particle capture efficiency by decreasing particle bounce (Huang et al. 2018), and particle liquid water may produce similar effects.

3.3. Effects of temperature and lights

In contrast to environmental RH and particle water, we found that chamber temperature did not significantly alter the wall loss profiles of AS (and presumably mixed AS) or sorbitol particles (Figure 3). While there is some deviation in the $\beta(D_p)$ profiles at lower particle diameters (up to 14% in the sorbitol case), the standard deviation for particles that highly affect total particle mass (i.e., D_p > 100 nm) is ~ 4% in both cases, well within the baseline uncertainty. Temperature may affect diffusion-controlled processes more than sedimentation, which supports a larger $\beta(D_p)$ profile variation for smaller diameter particles. However, we cannot rule out fitting uncertainties in this case either as the population of very small diameter particles tend to be much smaller than

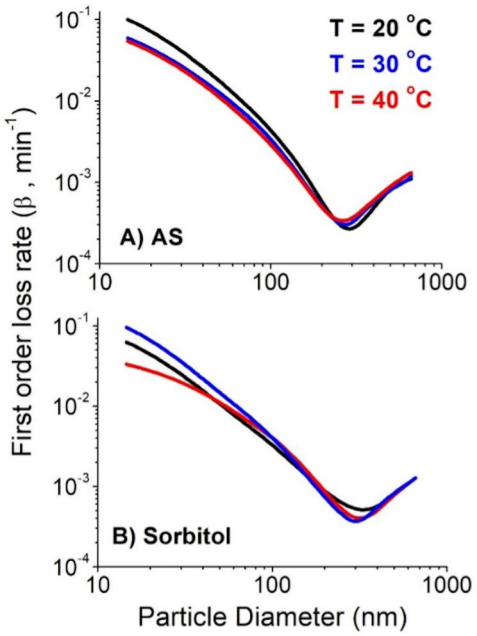

Figure 3. The $\beta(D_p)$ profile of sorbitol and ammonium sulfate (AS) particles at different temperatures and RH < 10% in the dark.

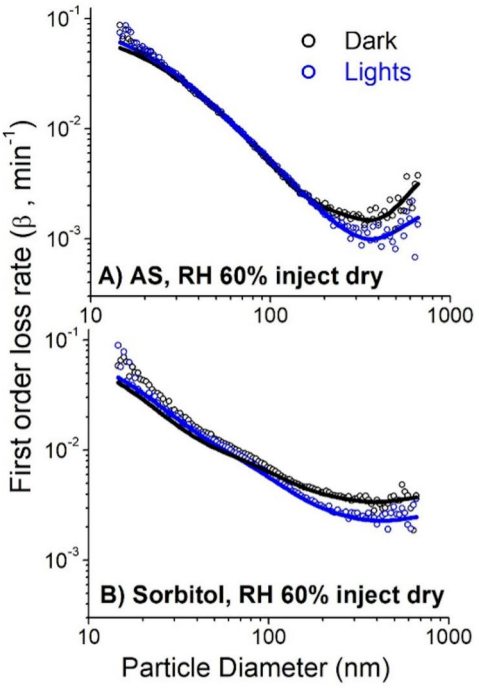

Figure 4. The $\beta(D_p)$ profile of sorbitol and ammonium sulfate (AS) particles at RH 60%, injected dry, in darkness (black) and with 100% chamber lights on (blue).

mid-range diameter particles, and thus, may affect statistics.

Chamber lights produced a small but noticeable effect on particle wall loss, likely because their emitted heat influences temperature and RH. Otherwise-identical experiments using dry-injected AS and sorbitol particles at RH ~60% but with the fluorescent UV lights turned on or off (Figure 4) showed deviations in wall loss profiles outside of the repeatability range (1σ deviations of 8–9% at all D_p, 13–14% at $D_p >$ 100 nm). Even with the use of a temperature control system, heat from the lights is not perfectly modulated throughout the enclosure such that the chamber experienced an increase of ~2 °C from lights and, thus, an RH decrease of ~5%. Given the minimal effects of temperature on $\beta(D_p)$ profiles (Figure 3), we attribute the decrease in wall loss rates when the lights are turned on to the subsequent decrease in RH. Typically, labs perform separate particle wall loss experiments in the dark, even when correcting for photolytically-initiated experiments. This practice is likely sound when RH is low, but at higher RH, additional errors may be introduced. Although the temperature and RH regulation effects from UV lights may be specific to our chamber, as a best practice we suggest that separate particle wall loss experiments should be performed in identical conditions with lights on, or that RH be adjusted to identical settings for the lights on and off scenarios.

3.4. Effects of chamber usage history

Of all the experimental parameters tested in this study (lights vs. dark, 20–40 °C, RH < 10–80%, and varied particle composition), chamber usage history affected particle wall loss rates most significantly (Figure 5). The particle wall loss experiments presented here were conducted contemporaneously with chemical experiments involving ozonolysis and nitrate radical (NO_3) oxidation of various terpenes (e.g., α- and β-pinene, ocimene, sabinene [Bates et al. 2022]) as well as photochemical experiments with sulfur dioxide (SO_2). During these experiments, the chamber walls were presumably contaminated with secondary organics with a range of functional groups (e.g., carbonyls, organic acids, organic nitrates, organic hydroperoxides), nitric acid from the aqueous uptake of N_2O_5, and sulfuric acid. Despite our adherence to standard flushing protocols (Bell, Doussin, and Hohaus 2023; Ma et al. 2022; Wu et al. 2007), we discovered that $\beta(D_p)$ profiles diverged considerably for particle wall loss experiments performed within 24 h after a chemical experiment ("dirty") compared to those conducted in a "clean" chamber (where clean indicates that the

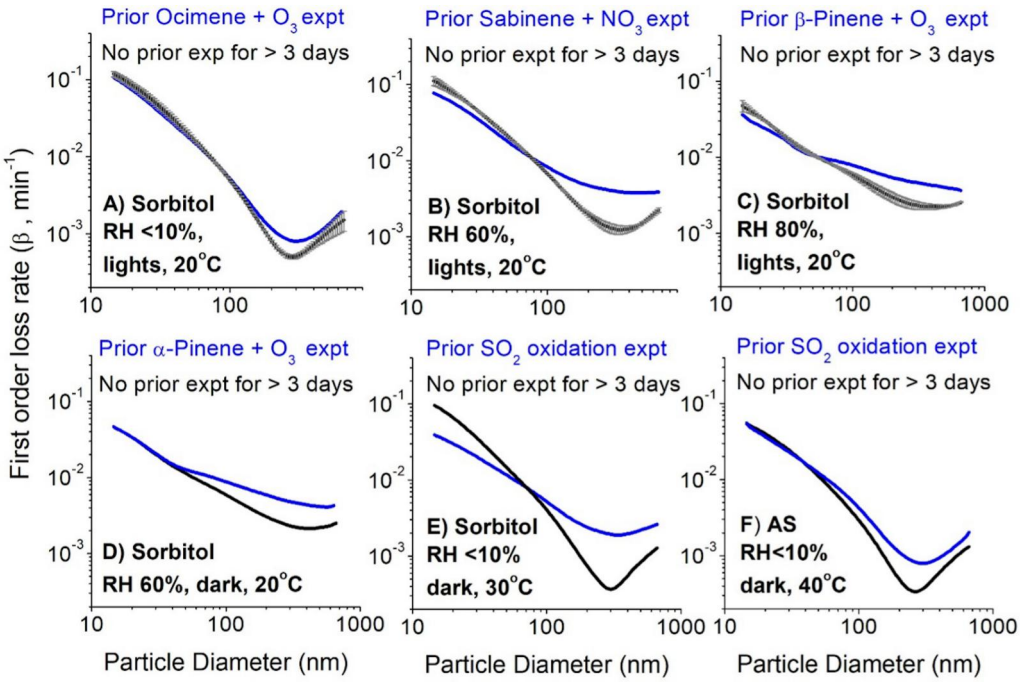

Figure 5. $\beta(D_p)$ profiles of sorbitol and ammonium sulfate (AS) particles at various conditions, comparing between wall loss experiments performed in a "clean" chamber (after oxidative cleaning and/or after flushing for > 3 days) and within 24 h of an oxidation experiment. Panels (a)–(c) feature repeated experiments done in the "clean" scenario, where the average $\beta(D_p)$ profiles are shown along with 1-σ standard deviation uncertainty bars in the y-direction.

chamber has either been photochemically cleaned or unused for more than 3 days with constant flushing). For all six scenarios presented in Figure 5, the clean (black trace) and dirty (blue trace) chamber conditions yield strikingly different loss profiles, and the 1σ error bars in panels a-c illustrate the magnitude of the discrepancies relative to the baseline uncertainty.

Evidently, the largest deviations in $\beta(D_p)$ profiles occur when the previous day's chemical experiment produced acids on the walls (NO_3 and SO_2 experiments), but more data are required to confirm if this is universally true. It is possible that hygroscopic compounds such as acids on the walls increase the water content at the surface of the Teflon film, which may lead to more efficient particle capture and reduced particle bounce on the walls. Nevertheless, it is clear that all prior chemical experiments introduced unacceptable levels of error into the $\beta(D_p)$ profiles that cannot be explained through baseline repeatability errors. Under dirty environmental chamber conditions we extracted loss profiles with standard deviations of 10–34% over the entire D_p range, and importantly, we observed deviations of 14–46% for $D_p > 100$ nm that contributes the most to particle volume and mass.

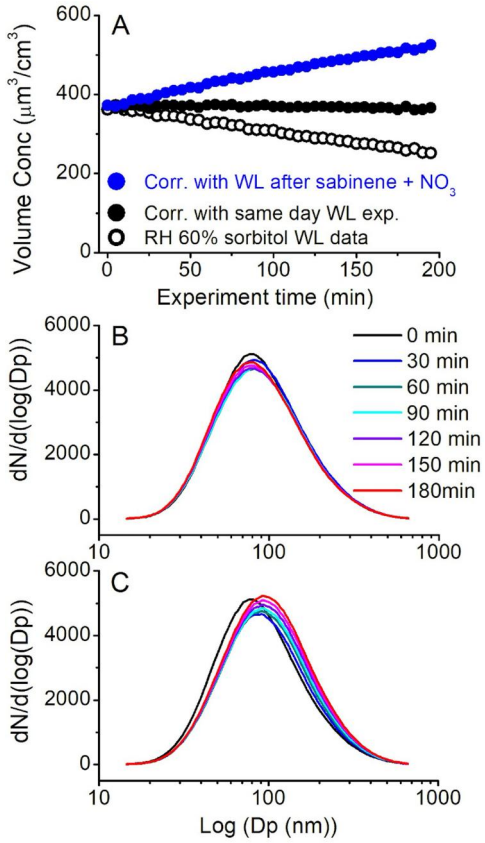

Figure 6. (a) Correction to particle volume data using the $\beta(D_p)$ profiles from Figure 5b, respectively: black open circles are the uncorrected wall loss (WL) data in a clean bag; black closed circles are data corrected with the black $\beta(D_p)$ profile in Figure 5b, which was obtained in a clean chamber with same day data; blue closed circles data corrected with the blue $\beta(D_p)$ profile in Figure 5b, which was obtained after a sabinene + NO_3 experiment. (b) The particle number distribution when corrected with the black $\beta(D_p)$ profile in Figure 5b. (c) The particle number distribution when corrected with the blue $\beta(D_p)$ profile in Figure 5b.

To understand the magnitude of the correction errors, we demonstrate the correction biases using sorbitol wall loss data obtained in clean and dirty chamber environments both at RH 60%, 20 °C, and with the UV lights on (Figure 5b). Figure 6a shows how the $\beta(D_p)$ profile extracted from a clean same-day wall loss experiment applies an acceptable correction to the particle volume concentration data. Conversely, under identical experimental conditions the $\beta(D_p)$ profile extracted from a dirty chamber (with a sabinene + NO_3 experiment performed within 24 h before the wall loss experiment) on a different day overcorrects the particle volume data by approximately 40% after 200 min, and the discrepancy in the correction grows with experiment time. While number concentration data only differ by 3% at the 200-min mark, the overcorrection from the dirty chamber $\beta(D_p)$ profile shifts the particle distribution to a higher mean D_p (Figure 6b and c), resulting in a much larger discrepancy in particle volume (and thus, mass). This is because the errors in particle D_p are amplified in a cubic manner when calculating volume and mass. These data highlight the importance of size-dependent particle wall loss corrections, as even minor deviations in the particle D_p distribution can cause major uncertainties when correcting particle volume and mass. In SOA experiments, it is possible that errors in particle wall loss corrections may also affect the trend of SOA time evolution in addition to the magnitude of mass concentration.

Chemistry experiments conducted in the same chamber within close time proximity of each other are routinely corrected with non-unique, standardized $\beta(D_p)$ profiles that neglect to account for the chamber's usage history at the time of experimentation. In our chamber, chemical experiments performed with different hydrocarbons or different oxidation chemistry require multiple days of flushing (approximately 30 volume exchanges) between each run and/or photochemical cleaning to be justifiably treated with the same standard $\beta(D_p)$ profile obtained in clean chamber conditions. Or, rather, wall loss profiles may need to be considered on a day-by-day basis, ideally by using a pre-experiment period after initial particle injection but prior to any chemical reaction to measure wall loss rates under the precise experimental conditions. It may

also be the case that deposition of gases and particles to chamber walls during an oxidation experiment induces sufficient surface contamination to change particle loss rates over the course of the experiment, in which case an additional post-experiment wall loss period would be necessary to fully characterize particle loss rates during the experiment.

4. Conclusions

Though particle wall loss in Teflon chambers is a well-documented phenomenon, there is limited consensus on the best practices for applying wall loss corrections, and our work implies a need to consider various experimental conditions when developing size-dependent loss profiles. Among the conditions investigated in our Teflon chamber (temperature, RH, particle hydration, lights, particle composition, and usage history), we found: (1) chamber temperature exerted little influence on wall loss profiles of both inorganic (AS) and organic (sorbitol) particles; (2) RH and particle liquid water significantly altered wall loss profiles for all tested compositions including mixed (AS + sorbitol) particles; (3) chamber lights had a minor effect, possibly *via* indirect effects on chamber RH and/or particle liquid water; and (4) chamber usage history with respect to chemical experiments had the most pronounced impact on wall losses for any particle composition under all tested conditions. In particular, these chamber usage findings recall the impacts of HONO and HNO_3 deposition from prior experiments on radical generation seen in early chamber experiments (Bufalini, Walter, and Bufalini 1977; Carter et al. 1982; Besemer and Nieboer 1985), and may also be connected to the history effects hypothesized for wall losses of vapors (Loza et al. 2010; Shao et al. 2022). Matsunaga and Ziemann (2010) compared vapor wall partitioning between a new Teflon chamber and one used with SOA experiments and found minimal differences between the two chambers; however, the SOA chamber in that work was routinely cleaned by exposure to light and oxidants, which would have removed the immediate chamber history effects shown here. We also show that the particle size dependence is highly important in wall loss correction considerations, as errors in the particle D_p distribution are amplified when calculating particle volume and mass.

Given the heterogeneity in chamber construction, operation, and usage histories, it may not be straightforward to extrapolate trends from our chamber to other facilities. Stainless steel and other chamber materials may have entirely different particle wall loss dependencies, although they exhibit similar wall loss size dependencies to Teflon chambers (Wang et al. 2011; Lamkaddam 2017; Massabò et al. 2018) and can similarly retain usage histories in the form of deposited organic compounds (Schnitzhofer et al. 2014). Still, we recommend that experimental characterizations of particle wall losses be performed under identical conditions that consider particle composition, particle water, environmental RH, wall usage history, and possibly illumination from artificial or natural lights. Alternatively, experimenters may wish to individually characterize the effects of RH, particle water content, and chamber usage history on particle wall loss rates in their own chambers, by conducting a similar set of experiments to those shown here in which one variable is changed at a time (e.g., a base particle wall loss experiment using dry AS at 60% RH in a clean chamber, followed by one identical experiment except at <10% RH, one with the particles injected wet, and one <24 h after an oxidation experiment). The approach of extracting particle wall loss rate profiles from the an initial 4 h period prior to the start of chemistry (Wang et al. 2018b) may be more accurate than many other approaches currently in practice, although this does not account for the possibility of particle wall loss rates changing due to deposition of particles and gases to the walls over the course of the experiment, or due to any other alteration to environmental conditions. For sensitive or precise particle experiments, experiments that survey many different chemical regimes and conditions, and experiments conducted over long timescales, extracting and comparing wall loss profiles both before and after an experiment could enable a more thorough characterization of particle loss rates.

Disclosure statement

The authors declare no competing interests.

Funding

We acknowledge funding from the National Science Foundation, Division of Atmospheric and Geospace Sciences, Atmospheric Chemistry Program under grant 1740571 and the California Agricultural Experiment Station grant CAD-ETX-2699-H through the USDA National Institute of Food and Agriculture.

ORCID

Kelvin H. Bates http://orcid.org/0000-0001-7544-9580
Tran B. Nguyen http://orcid.org/0000-0001-9206-4359

Data availability statement

Chamber experiment data are available online at the Integrated Chamber Atmospheric data Repository for Unified Science (ICARUS): https://icarus.ucdavis.edu/experimentset/265.

References

Bates, K. H., G. J. P. Burke, J. D. Cope, and T. B. Nguyen. 2022. Secondary organic aerosol and organic nitrogen yields from the nitrate radical (NO3) oxidation of alpha-pinene from various RO_2 fates. *Atmos. Chem. Phys.* 22 (2):1467–82. doi:10.5194/acp-22-1467-2022.

Bell, D., J.-F. Doussin, and T. Hohaus. 2023. Preparation of simulation chambers for experiments. In *A practical guide to atmospheric simulation chambers*, ed. J.-F. Doussin, H. Fuchs, A. Kiendler-Scharr, P. Seakins, J. Wegner. Cham, Switzerland: Springer International Publishing. doi:10.1007/978-3-031-22277-1_3.

Besemer, A. C., and H. Nieboer. 1985. The wall as a source of hydroxyl radicals in smog chambers. *Atmos. Environ.* 19 (3):507–13. doi:10.1016/0004-6981(85)90171-4.

Biskos, G., L. M. Russell, P. R. Buseck, and S. T. Martin. 2006. Nanosize effect on the hygroscopic growth factor of aerosol particles. *Geophys. Res. Lett.* 33 (7):L07801. doi:10.1029/2005GL025199.

Bufalini, J. J., T. A. Walter, and M. M. Bufalini. 1977. Contamination effects on ozone formation in smog chambers. *Environ. Sci. Technol.* 11 (13):1181–5. doi:10.1021/es60136a009.

Carter, W. P. L., R. Atkinson, A. M. Winer, and J. N. Pitts. Jr. 1982. Experimental investigation of chamber-dependent radical sources. *Int. J. Chem. Kinetics* 14 (10):1071–103. doi:10.1002/kin.550141003.

Charan, S. M., W. Kong, R. C. Flagan, and J. H. Seinfeld. 2018. Effect of particle charge on aerosol dynamics in teflon environmental chambers. *Aerosol. Sci. Technol.* 52 (8):854–71. doi:10.1080/02786826.2018.1474167.

Chen, B. T., H. C. Yeh, and Y. S. Cheng. 1992. Evaluation of an environmental reaction chamber. *Aerosol Sci. Technol.* 17 (1):9–24. doi:10.1080/02786829208959556.

Corner, J., and E. D. Pendlebury. 1951. The coagulation and deposition of a stirred aerosol. *Proc. Phys. Soc. B* 64 (8):645–54. doi:10.1088/0370-1301/64/8/304.

Crump, J. G., and J. H. Seinfeld. 1981. Turbulent deposition and gravitational sedimentation of an aerosol in a vessel of arbitrary shape. *J. Aerosol Sci.* 12 (5):405–15. doi:10.1016/0021-8502(81)90036-7.

Crump, J. G., R. C. Flagan, and J. H. Seinfeld. 1982. Particle wall loss rates in vessels. *Aerosol. Sci. Technol.* 2 (3):303–9. doi:10.1080/02786828308958636.

Emerson, E. W., A. L. Hodshire, H. M. DeBolt, K. R. Bilsback, J. R. Pierce, G. R. McMeeking, and D. K. Farmer. 2020. Revisiting particle dry deposition and its role in radiative effect estimates. *Proc. Natl. Acad. Sci. U. S. A.* 117 (42):26076–82. doi:10.1073/pnas.2014761117.

Fry, J. L., D. C. Draper, K. C. Barsanti, J. N. Smith, J. Ortega, P. M. Winkler, M. J. Lawler, S. S. Brown, P. M. Edwards, R. C. Cohen, et al. 2014. Secondary organic aerosol formation and organic nitrate yield from NO_3 oxidation of biogenic hydrocarbons. *Environ. Sci. Technol.* 48 (20):11944–53. doi:10.1021/es502204x.

Hennigan, C. J., M. A. Miracolo, G. J. Engelhart, A. A. May, A. A. Presto, T. Lee, A. P. Sullivan, G. R. McMeeking, H. Coe, C. E. Wold, et al. 2011. Chemical and physical transformations of organic aerosol from the photo-oxidation of open biomass burning emissions in an environmental chamber. *Atmos. Chem. Phys.* 11 (15):7669–86. doi:10.5194/acp11-7669-2011.

Henry, K. M., and N. M. Donahue. 2012. Photochemical aging of α-pinene secondary organic aerosol: Effects of OH radical sources and photolysis. *J. Phys. Chem. A* 116 (24):5932–40. doi:10.1021/jp210288s.

Hildebrandt, L., N. M. Donahue, and S. N. Pandis. 2009. High formation of secondary organic aerosol from the photo-oxidation of toluene. *Atmos. Chem. Phys.* 9 (9):2973–86. doi:10.5194/acp-9-2973-2009.

Huang, Y., R. Zhao, S. M. Charan, C. M. Kenseth, X. Zhang, and J. H. Seinfeld. 2018. Unified theory of vapor-wall mass transport in teflon-walled environmental chambers. *Environ. Sci. Technol.* 52 (4):2134–42. doi:10.1021/acs.est.7b05575.

Ingebrethsen, B. J., and S. B. Sears. 1989. Particle Evaporation of Sidestream Tobacco Smoke in a Stirred Tank. *J. Colloid Interface Sci.* 131 (2):526–36. doi:10.1016/0021-9797(89)90195-1.

Keywood, M. D., V. Varutbangkul, R. Bahreini, R. C. Flagan, and J. H. Seinfeld. 2004. Secondary organic aerosol formation from the ozonolysis of cycloalkenes and related compounds. *Environ. Sci. Technol.* 38 (15):4157–64. doi:10.1021/es035363o.

Kim, M., S.-G. Jeong, J. Park, S. Kim, and J.-H. Lee. 2023. Investigating theimpact of relative humidity and air tightness on PM sedimentation and concentration reduction. *Buil. Environ.* 241:110270. doi:10.1016/j.buildenv.2023.110270.

Lamkaddam, H. 2017. *Study under simulated condition of the secondary organic aerosol from the photooxydation of n-dodecane: Impact of the physical-chemical processes.* Créteil, France: Université Paris-Est.

Loza, C. L., A. W. H. Chan, M. M. Galloway, F. N. Keutsch, R. C. Flagan, and J. H. Seinfeld. 2010. Characterization of vapor wall loss in laboratory chambers. *Environ. Sci. Technol.* 44 (13):5074–8. doi:10.1021/es100727v.

Loza, C. L., P. S. Chhabra, L. D. Yee, J. S. Craven, R. C. Flagan, and J. H. Seinfeld. 2012. Chemical aging of m-xylene secondary organic aerosol: Laboratory chamber study. *Atmos. Chem. Phys.* 12 (1):151–67. doi:10.5194/acp-12-151-2012.

Ma, W., Y. Liu, Y. Zhang, Z. Feng, J. Zhan, C. Hua, L. Ma, Y. Guo, Y. Zhang, W. Zhou, et al. 2022. A new type of quartz smog chamber: Design and characterization. *Environ. Sci. Technol.* 56 (4):2181–90. doi:10.1021/acs.est.1c06341.

Massabò, D., S. G. Danelli, P. Brotto, A. Comite, C. Costa, A. Di Cesare, J. F. Doussin, F. Ferraro, P. Formenti, E. Gatta, et al. 2018. ChAMBRe: A new atmospheric simulation chamber for aerosol modelling and bio-aerosol research. *Atmos. Meas. Tech.* 11 (10):5885–900. doi:10.5194/amt-11-5885-2018.

Matsunaga, A., and P. J. Ziemann. 2010. Gas-wall partitioning of organic compounds in a Teflon film chamber and potential effects on reaction product and aerosol yield measurements. *Aerosol Sci. Tech.* 44 (10):881–92. doi:10.1080/02786826.501044.

McMurry, P. H., and D. Grosjean. 1985. Gas and aerosol wall losses in teflon film smog chambers. *Environ. Sci. Technol.* 19 (12):1176–82. doi:10.1021/es00142a006.

McMurry, P. H., and D. J. Rader. 1985. Aerosol wall losses in electrically charged chambers. *Aerosol Sci. Tech.* 4 (3): 249–68. doi:10.1080/02786828508959054.

Nah, T., R. C. McVay, J. R. Pierce, J. H. Seinfeld, and N. L. Ng. 2017. Constraining uncertainties in particle-wall deposition correction during soa formation in chamber experiments. *Atmos. Chem. Phys.* 17 (3):2297–310. doi:10.5194/acp-17-2297-2017.

Ng, N. L., J. H. Kroll, A. W. H. Chan, P. S. Chhabra, R. C. Flagan, and J. H. Seinfeld. 2007. Secondary organic aerosol formation from m-xylene, toluene, and benzene. *Atmos. Chem. Phys.* 7 (14):3909–22. doi:10.5194/acp-7-3909-2007.

Offermann, F. J., R. G. Sextro, W. J. Fisk, D. T. Grimsrud, W. W. Nazaroff, A. V. Nero, K. L. Revzan, and J. Yater. 1985. Control of respirable particles in indoor air with portable air cleaners. *Atmos. Environ.* 19 (11):1761–71. doi:10.1016/0004-6981(85)90003-4.

Okuyama, K., Y. Kousaka, S. Yamamoto, and T. Hosokawa. 1986. Particle loss of aerosols with particle diameters between 6 and 2000 nm in stirred Tank. *J. Colloid Interface Sci.* 110 (1):214–23. doi:10.1016/0021-9797(86)90370-X.

Okuyama, K., Y. Kousaka, Y. Kida, and T. Yoshida. 1977. Turbulent coagulation of aerosols in a stirred tank. *J. Chem. Eng. Jpn.* 10 (2):142–7. doi:10.1252/jcej.10.142.

Pandian, M. D., and S. K. Friedlander. 1988. Particle deposition to smooth and rough walls of stirred chambers: Mechanisms and engineering correlations. *PCH Physico Chem. Hydrodyn* 10:639–45.

Park, S. H., H. O. Kim, Y. T. Han, S. B. Kwon, and K. W. Lee. 2001. Wall loss rate of polydispersed aerosols. *Sci. Technol* 35 (3):710–7. doi:10.1080/02786820152546752.

Parsons, M. T., D. A. Knopf, and A. K. Bertram. 2004. Deliquescence and crystallization of ammonium sulfate particles internally mixed with water-soluble organic compounds. *J. Phys. Chem. A* 108 (52):11600–8. doi:10.1021/jp0462862.

Pathak, R. K., C. O. Stanier, N. M. Donahue, and S. N. Pandis. 2007. Ozonolysis of a-pinene at atmospherically relevant concentrations: Temperature dependence of aerosol mass fractions (yields). *J. Geophys. Res.* 112 (D3): D03201. doi:10.1029/2006JD007436.

Peng, C., A. H. Chow, and C. K. Chan. 2001. Hygroscopic study of glucose, citric acid, and sorbitol using an electrodynamic balance: Comparison with unifac predictions. *Aerosol Sci. Technol.* 35 (3):753–8. doi:10.1080/02786820152546798.

Pierce, J. R., G. J. Engelhart, L. Hildebrandt, E. A. Weitkamp, R. K. Pathak, N. M. Donahue, A. L. Robinson, P. J. Adams, and S. N. Pandis. 2008. Constraining particle evolution from wall losses, coagulation, and condensation-evaporation in smog chamber experiments: Optimal estimation based on size distribution measurements. *Aerosol Sci. Tech.* 42 (12): 1001–15. doi:10.1080/02786820802389251.

Reid, J. P., A. K. Bertram, D. O. Topping, A. Laskin, S. T. Martin, M. D. Petters, F. D. Pope, and G. Rovelli. 2018. The viscosity of atmospherically relevant organic particles. *Nat. Comm.* 9:956.

Schnitzhofer, R., A. Metzger, M. Breitenlechner, W. Jud, M. Heinritzi, L.-P. De Menezes, J. Duplissy, R. Guida, S. Haider, J. Kirkby; the CLOUD Team, et al. 2014. Characterisation of organic contaminants in the CLOUD chamber at CERN. *Atmos. Meas. Tech.* 7 (7):2159–68. and doi:10.5194/amt-7-2159-2014.

Schwantes, R. H., S. M. Charan, K. H. Bates, Y. Huang, T. B. Nguyen, H. Mai, W. Kong, R. C. Flagan, and J. H. Seinfeld. 2019. Low-volatility compounds contribute significantly to isoprene secondary organic aerosol (SOA) under high-NO_x conditions. *Atmos. Chem. Phys.* 19 (11): 7255–78. doi:10.5194/acp-19-7255-2019.

Shao, Y., Y. Wang, M. Du, A. Voliotis, M. R. Alfarra, S. P. O'Meara, S. F. Turner, and G. McFiggans. 2022. Characterisation of the manchester aerosol chamber facility. *Atmos. Meas. Tech.* 15 (2):539–59. doi:10.5194/amt-15-539-2022.

Stern, J. E., R. C. Flagan, D. Grosjean, and J. H. Seinfeld. 1987. Aerosol formation and growth in atmospheric aromatic hydrocarbon photooxidation. *Environ. Sci. Technol.* 21 (12):1224–31. doi:10.1021/es00165a011.

Takekawa, H., H. Minoura, and S. Yamazaki. 2003. Temperature dependence of secondary organic aerosol formation by photo-oxidation of hydrocarbons. *Atmos. Environ.* 37 (24):3413–24. doi:10.1016/S1352-2310(03)00359-5.

Wang, J., J. F. Doussin, S. Perrier, E. Perraudin, Y. Katrib, E. Pangui, and B. Picquet-Varrault. 2011. Design of a new multi-phase experimental simulation chamber for atmospheric photosmog, aerosol and cloud chemistry research. *Atmos. Meas. Tech.* 4 (11):2465–94. doi:10.5194/amt-4-2465-2011.

Wang, X., T. Liu, F. Bernard, X. Ding, S. Wen, Y. Zhang, Z. Zhang, Q. He, S. Lü, J. Chen, et al. 2014. Design and characterization of a smog chamber for studying gas-phase chemical mechanisms and aerosol formation. *Atmos. Meas. Tech.* 7 (1):301–13. doi:10.5194/amt-7-301-2014.

Wang, N., S. D. Jorga, J. R. Pierce, N. M. Donahue, and S. N. Pandis. 2018a. Particle wall-loss correction methods in smog chamber experiments. *Atmos. Meas. Tech.* 11 (12):6577–88. doi:10.5194/amt-11-6577-2018.

Wang, N., E. Kostenidou, N. M. Donahue, and S. N. Pandis. 2018b. Multi-generation chemical aging of α-pinene ozonolysis products by reactions with OH. *Atmos. Chem. Phys.* 18 (5):3589–601. doi:10.5194/acp-18-3589-2018.

Weitkamp, E. A., A. M. Sage, J. R. Pierce, N. M. Donahue, and A. L. Robinson. 2007. Organic aerosol formation from photochemical oxidation of diesel exhaust in a smog chamber. *Environ. Sci. Technol.* 41 (20):6969–75. doi:10.1021/es070193r.

Wu, S., Z. Lü, J. Hao, Z. Zhao, J. Li, H. Takekawa, H. Minoura, and A. Yasuda. 2007. Construction and characterization of an atmospheric simulation smog chamber. *Adv. Atmos. Sci.* 24 (2):250–8. doi:10.1007/s00376-007-0250-3.